

# Safety Verification of Seismic Isolation Systems Using Elasto-plastic Dampers against Long-period Earthquake Motions



**S. Yamamoto, T. Nishimura & K. Nakanishi**

*Shimizu Corporation, Tokyo, Japan*

**M. Hikita & Y. Takenaka**

*Kajima Corporation, Tokyo, Japan*

**M. Takayama**

*Fukuoka University, Fukuoka, Japan*

**M. Kikuchi**

*Hokkaido University, Hokkaido, Japan*

**M. Iiba**

*Building Research Institute, Ibaraki, Japan*

## SUMMARY:

In recent years, long-period ground motions caused by subduction-zone earthquakes and their impact on super high-rise buildings and seismically isolated buildings have been attracting considerable attention in Japan. The safety of seismic isolation systems against long-period earthquake motions must be verified urgently because it is estimated that an earthquake with long-period ground motions may occur in the near future. In order to investigate the performance of seismic isolation devices against long-period earthquake motions, we have conducted multi-cyclic loading tests of full-scale elasto-plastic dampers used for seismic isolation systems. We employed two types of damper, steel dampers and lead dampers. Static tests were carried out for the steel dampers and dynamic tests were performed for the lead dampers. As a result of the tests, variations in shear strength, energy dissipation capability and the low-cycle fatigue characteristics of the steel dampers and the lead dampers were confirmed.

*Keywords: Seismic Isolation, Long-period Earthquake Motions, Elasto-plastic Damper, Multi-cyclic shear test*

## 1. INTRODUCTION

The 2011 Earthquake off the Pacific coast of Tohoku brought about long-period ground motions in the Kanto plain, which shook super high-rise buildings as well as seismically isolated buildings for a long duration of more than several minutes. It is estimated that a Tokai, Tonankai, Nankai earthquake or an earthquake which combines these may occur in the near future and the Kanto, Nobi and Osaka plains will be exposed to long-period ground motions of large amplitudes. This prediction has led to growing public concern with the safety of seismic isolation systems against long-period earthquake motions in Japan. Since earthquakes with long-period ground motions bring large amounts of energy to seismically isolated buildings, the isolation devices which are expected to absorb most of the input energy are required to have a large energy dissipation capability. In order to verify the safety of isolated buildings against long-period ground motions, it is necessary to evaluate the performance of seismic isolation devices under multi-cyclic shear deformations of large amplitudes. However, the hysteretic characteristics of seismic isolation devices up to their fracture under multi-cyclic deformations are not well understood. To investigate the performance of seismic isolation devices under multi-cyclic shear deformations, we conducted multi-cyclic shear loading tests of seismic isolation devices. In this paper, we report the test results for two types of elasto-plastic dampers, steel dampers and lead dampers, which are generally used in seismic isolation systems as energy dissipation components. The variations in hysteretic properties with multi-cyclic loading and the low-cycle fatigue characteristics of these two types of damper are examined.

## 2. MULTI-CYCLIC SHEAR TESTS FOR STEEL DAMPERS

### 2.1. Steel Damper Tests

The specimens are U-shaped steel dampers named NSUD55×4. Four specimens were tested. Fig. 2.1 shows the design of the steel dampers. The steel dampers are combinations of four 45 mm thick U-shaped steel rods. Two rods were attached to the flange plates at a direction of 0 degrees, parallel to the loading direction, and the other two rods were attached at a direction of 90 degrees, orthogonal to the loading direction. Basic properties of the steel dampers are shown in Table 2.1. A schematic drawing of the testing Machine used for the steel damper tests is shown in Fig. 2.2. The horizontal force, displacement and temperature of one specimen during loading were measured. The thermometer installation points (four points) are shown in Fig. 2.1. Insulators against heat, which are 10 mm thick boards, were set between the testing machine and upper and lower flange plates of the steel damper. The insulators prevent the heat in the steel dampers generated by multi-cyclic loading from being carried to the testing machine.

The loading program is shown in Table 2.2. The tests consisted of fully reversed cycles of triangular horizontal displacement-controlled loading. The loadings were continued until three damper rods were broken or until the loading was repeated twice the number of cycles at the first rod broken. Since steel dampers have little velocity dependency, static loading at a loading velocity of 10 mm/s was conducted. Two types of multi-cyclic loading was performed. One was a multi-cyclic test with a constant shear deformation amplitude, and the other was a multi-cyclic test with a varying shear deformation amplitude. Specimens 1 and 2 were tested with constant shear deformation amplitudes of 100 mm and 400 mm, respectively. Specimens 3 and 4 were tested with varying shear deformation amplitudes. The number of cycles at each amplitude in the tests with varying deformation amplitudes was determined based on the evaluation of low-cycle fatigue damage. The number of fully reversed cycles until the specimen achieves its fracture,  $N_f$ , is calculated from the following equation:

$$\delta = 0.0658N_f^{-0.15} + 6.81N_f^{-0.80} \quad (2.1)$$

where  $\delta$  (m) is shear deformation amplitude. Eqn. 2.1 is derived from Manson-Coffin equations [1]. Using Eqn. 2.1,  $N_f = 294, 100, 58$  and  $38$  in the case of  $\delta = 0.1$  m,  $0.2$  m,  $0.3$  m and  $0.4$  m, respectively. In the tests with varying deformation amplitudes, the ratio of fatigue damage to their fracture at each amplitudes,  $0.1, 0.2, 0.3$  and  $0.4$  m, was  $5:2:2:1$  (pattern A) for specimen 3 and  $1:2:2:5$  (pattern B) for specimen 4 and the number of cycles at each amplitudes was calculated as follows:

$$294 \times \frac{5}{10} : 100 \times \frac{2}{10} : 58 \times \frac{2}{10} : 38 \times \frac{1}{10} \cong 38 : 5 : 3 : 1 \quad (\text{Pattern A}) \quad (2.2)$$

$$294 \times \frac{1}{10} : 100 \times \frac{2}{10} : 58 \times \frac{2}{10} : 38 \times \frac{5}{10} \cong 3 : 2 : 1 : 2 \quad (\text{Pattern B}) \quad (2.3)$$

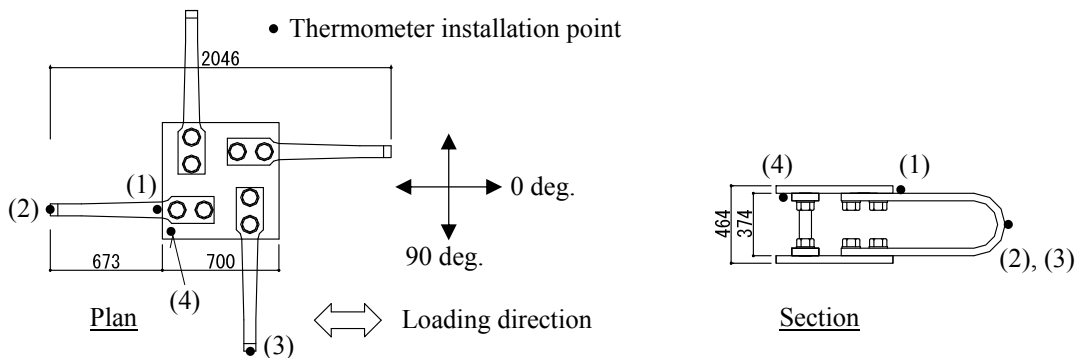
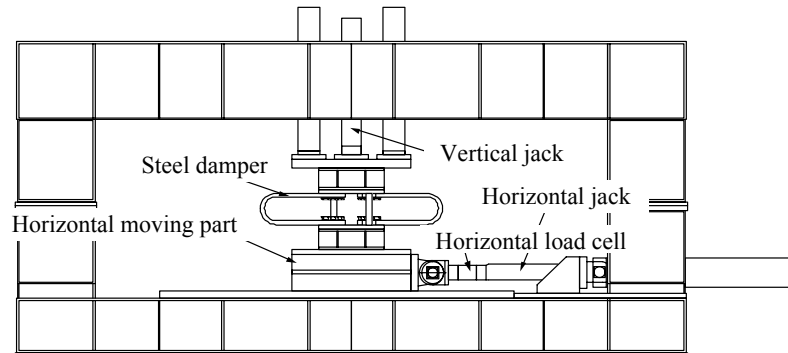


Figure 2.1. U-shaped steel damper design tested

**Table 2.1.** Basic properties of steel dampers tested

Initial stiffness	9,600 kN/m
Secondary stiffness	160 kN/m
Yield shear strength	304 kN
Maximum deformations of elasticity	31.7 mm
Maximum deformations of use	850 mm

**Figure 2.2.** Testing machine used for the steel damper tests**Table 2.2.** Loading program of steel damper tests

Specimen No.	Cyclic loading program
1	Constant shear deformation amplitude of 100 mm
2	Constant shear deformation amplitude of 400 mm
3	Varying shear deformation amplitudes in pattern A (100mm×38times - 200mm×5times - 300mm×3times - 400mm×1time)
4	Varying shear deformation amplitudes in pattern B (100mm×3times - 200mm×2times - 300mm×1time - 400mm×2times)

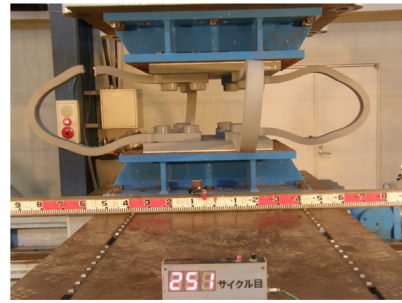
## 2.2. Test Results of the Steel Dampers

In all the tests, three damper rods of the specimens were broken. Two damper rods in the direction of 0 degrees were broken successively and a damper rod in the direction of 90 degrees was broken afterwards. The appearance of the specimens 2 and 3 at the time the first rod was broken are shown in Photograph 2.1. The hysteresis loops obtained from the cyclic loading tests with constant shear deformation amplitude for specimens 1 and 2 and with varying shear deformation amplitude for specimens 3 and 4 are shown in Fig. 2.3 and Fig. 2.4, respectively. The hysteresis loops show a gradual decline in the peak shear forces with the increase in the number of cycles. The peak shear force in the hysteresis loops decreased greatly whenever a steel damper rod was broken. However, the steel dampers exhibited stable behaviour up to their fracture. The temperatures of the steel rods and the flange plate of specimen 2 during loading were measured. The temperatures on all measured points were about 20 degrees at the time the test was started. The temperature on the points (2) and (3) (shown in Fig. 2.1) were about 80 degrees when the first rod broke. The temperature on the point (3) rose to 105 degrees by the cyclic loading up to the breakage of the third rod.

Fig. 2.5 shows variations in the amount of absorbed energy with the cyclic loading for specimens 2 and 3. From Fig. 2.5 (a), the absorbed energy per one cycle in the test of constant shear deformation amplitude gradually decreased with the increase in the number of cycles. The amount of absorbed energy at the first rod broken was 85% for that at the second cycle of this test. When the second rod was broken, the amount of absorbed energy was 45% for that at the second cycle of the test. The accumulative absorbed energy of both specimens 2 and 3 kept increasing during the loading and the increase rate of accumulative energy became gradual when a damper rod was broken.

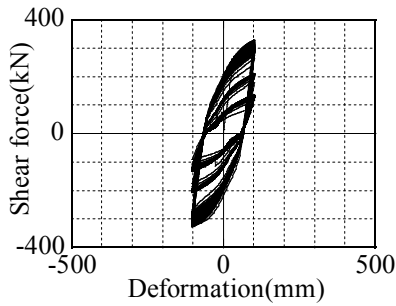


(a) Specimen 2

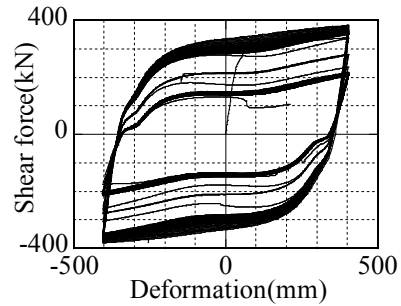


(b) Specimen 3

**Photograph 2.1.** Appearance of specimens 2 and 3 at the time the first rod was broken

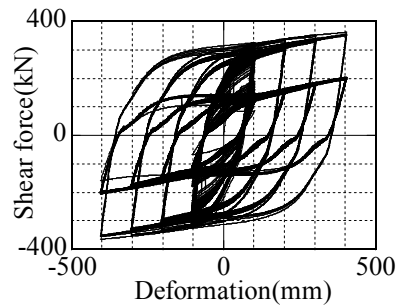


(a) Shear deformation amplitude of 100 mm

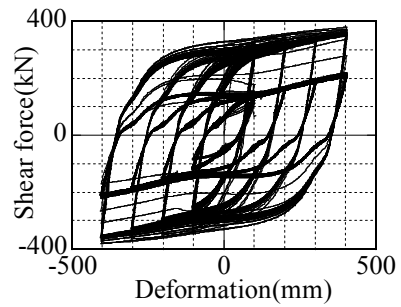


(b) Shear deformation amplitude of 400 mm

**Figure 2.3.** Experimental shear hysteresis loops for steel dampers cyclic shear loading with constant amplitude

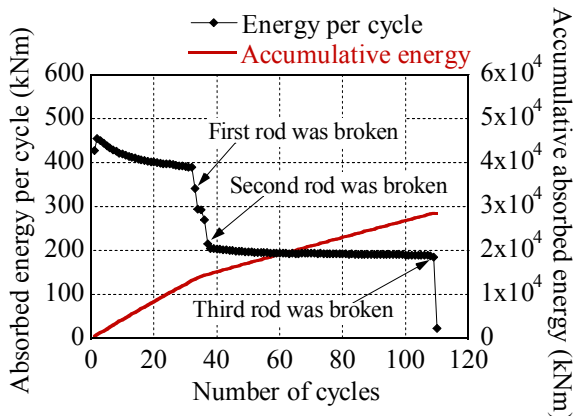


(a) Shear deformation amplitudes of 100mm×38, 200mm×5, 300mm×3 and 400mm×1

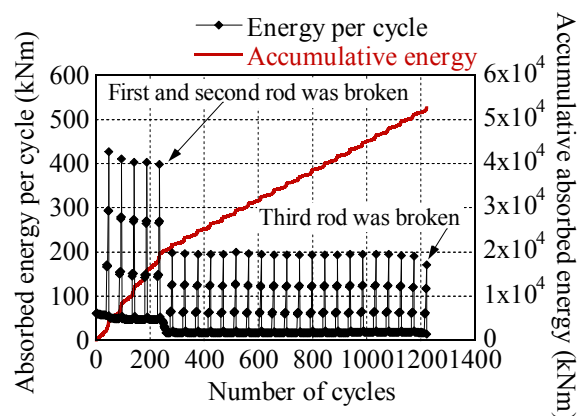


(b) Shear deformation amplitudes of 100mm×3, 200mm×2, 300mm×1 and 400mm×2

**Figure 2.4.** Experimental shear hysteresis loops for steel dampers cyclic shear loading with varying amplitude



(a) Specimen 2 (Constant deformation amplitude)



(b) Specimen 3 (Varying deformation amplitude)

**Figure 2.5.** Variation of the amount of absorbed energy with cyclic loading for the steel dampers

### 2.3. Fatigue Characteristics of Steel Dampers

In this section, the cumulative fatigue damage of the steel damper rods in the direction of 0 degrees is evaluated. Fig. 2.6 shows the evaluation curve expressed by Eqn. 2.1 and the number of cycles until breakage obtained from the test results. In the case of varying deformation amplitude, the number of cycles until breakage at each amplitude is plotted. The results of constant deformation amplitude show good agreement with the evaluation curve. Using Miner's rule [2],  $D$ , which expresses cumulative fatigue damage, is calculated from the following equation:

$$D = \sum D_i = \sum n_i / N_{fi} \tag{2.4}$$

where  $n_i$  and  $N_{fi}$  is number of cycles until breakage at a certain deformation amplitude obtained from the test results and calculated from Eqn. 2.1, respectively. The values of  $D$  calculated from Eqn. 2.4 are shown in Table 2.3. The values of  $D$  are about 1.0 in the case of varying deformation amplitude as well as in the case of constant deformation amplitude. This result indicates that the number of cycles until breakage of the steel damper in the case of varying deformation amplitude can be predicted by existing expressions for cumulative fatigue damage and Miner's rule.

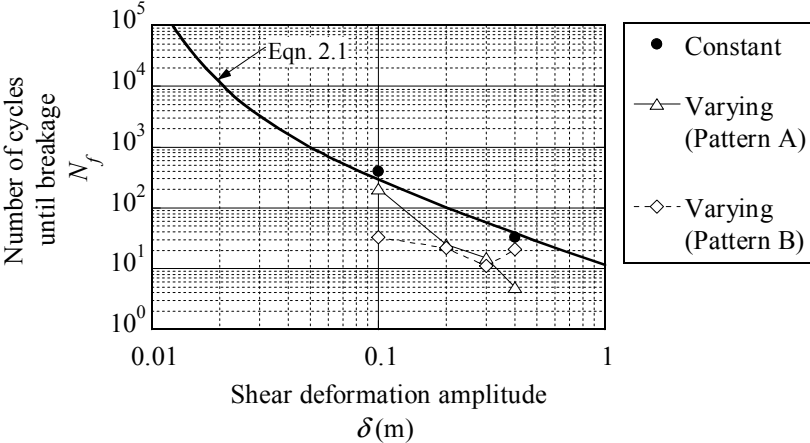


Figure 2.6. Comparison of the evaluation curve for fatigue characteristics (Eqn. 2.1) and the test results

Table 2.3. Comparison of the fatigue limit obtained from the test results and evaluated by the existing formula

Specimen No.	Deformation amplitude		$N_{fi}$	Number of cycles until breakage			
				First rod		Second rod	
				$n_i$	$D (= n_i / N_{fi})$	$n_i$	$D (= n_i / N_{fi})$
1	Constant	100 mm	294	404	<b>1.37</b>	447	<b>1.52</b>
2	Constant	400 mm	38	33	<b>0.87</b>	37	<b>0.97</b>
3	Varying (pattern A)	100 mm	294	206	0.70	213	0.72
		200 mm	100	25	0.25	25	0.25
		300 mm	59	15	0.25	15	0.25
		400 mm	38	5	0.13	5	0.13
					251	<b>1.34</b>	258
4	Varying (pattern B)	100 mm	294	33	0.11	34	0.12
		200 mm	100	22	0.22	22	0.22
		300 mm	59	11	0.19	11	0.19
		400 mm	38	21	0.55	22	0.58
					87	<b>1.07</b>	89

### 3. MULTI-CYCLIC TESTS OF LEAD DAMPERS

#### 3.1. Lead Damper Tests

The lead dampers tested are shown in Fig. 3.1. The specimens were full-scale lead dampers named U2426. Basic properties of the lead dampers are that their initial stiffness is 30,000 kN/m, secondary stiffness is 0, yield shear strength is 220 kN and yield shear deformation is 7.33 mm. Three specimens were tested. A schematic drawing of the testing machine used for the lead damper tests is shown in Fig. 3.2. Horizontal displacements were given to the upper flange of the lead dampers by an actuator via a loading beam. Insulators against heat, which are 10 mm thick boards, were set between the testing machine and upper and lower flange plates of the lead damper. Horizontal force, horizontal displacement and vertical displacement were measured.

The loading program is shown in Table 3.1. The tests consisted of sinusoidal horizontal loading and random horizontal loading. The loading directions, P and O, are shown in Fig. 3.1. Sinusoidal loading at shear deformation amplitudes of 100, 200 and 400 mm in the direction of P was conducted for specimen 1. Sinusoidal loading at a shear deformation amplitude of 150 mm in the direction of P and O by turns were performed for specimen 2. Specimen 3 was given response displacement motions, named EQ-T-TN, at the isolation layer obtained by a seismic time-history analysis. One-mass model supported by a lead damper and a natural rubber bearing was used for the seismic response analysis. The earthquake ground motion used for the time-history analysis was estimated as a long-period ground motion in the Nobi plain caused by the hypothetical Tokai-Tonankai earthquake. The duration of the estimated ground motion is over 600 seconds. We used a 150 seconds wave, from 60 to 210 s, of this wave that includes the principal motion of the predicted earthquake. Fig. 3.3 shows the response displacement wave used for the test. In the random horizontal loading test, twelve times the loading at response displacement motions were given to specimen 3. There was a short interval of three minutes between the third time loading and fourth time loading.

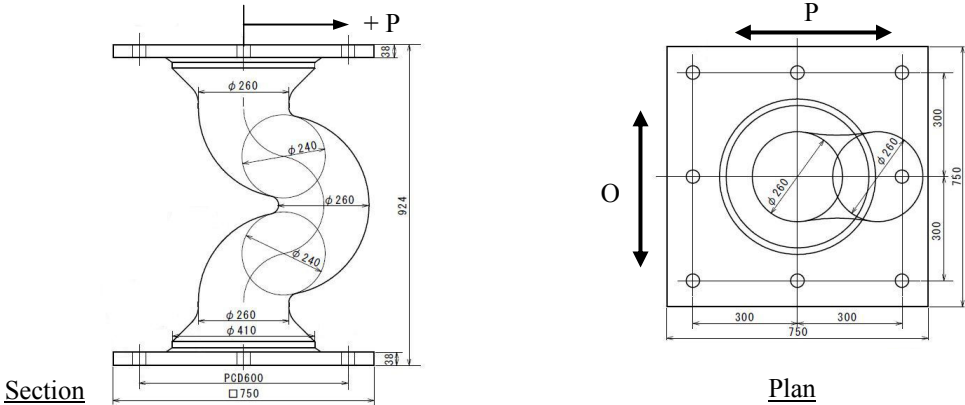


Figure 3.1. Lead damper design tested

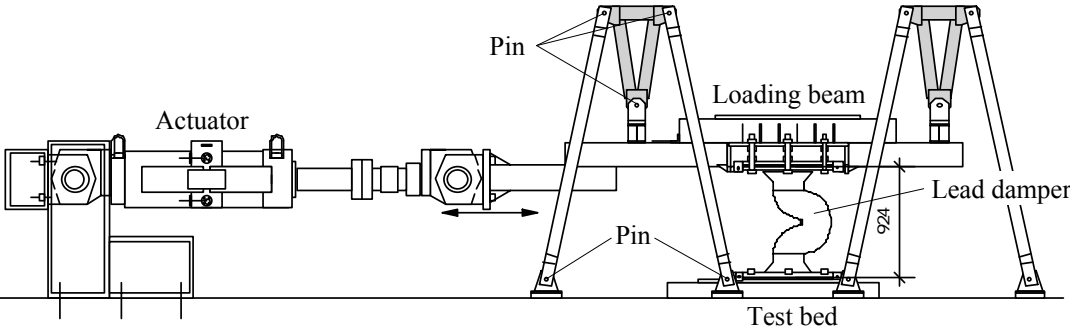
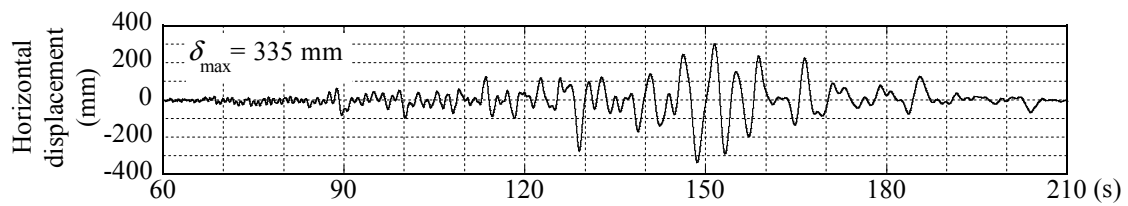


Figure 3.2. Testing machine used for the lead damper tests

**Table 3.1.** Loading program of the lead damper tests

Specimen No.	Test case	Loading period	Loading direction	Deformation amplitude	Number of cycles	Accumulative deformation
1	Sinusoidal loading in same direction	4.0 s	P	100 mm	30	12 m
		4.0 s		200 mm	30	36 m
		5.0 s		400 mm	Until breakage	50.9 m
2	Sinusoidal loading in different direction	4.0 s	P	150 mm	30	24 m
		4.0 s	O	150 mm	30	48 m
		4.0 s	P	150 mm	Until breakage	192.4 m
3	Response displacement of earthquake motion		P	EQ-T-TN 3 times		42 m
				Interval 3 min.		
				EQ-T-TN 9 times		168 m

**Figure 3.3.** Response displacement used for the random loading

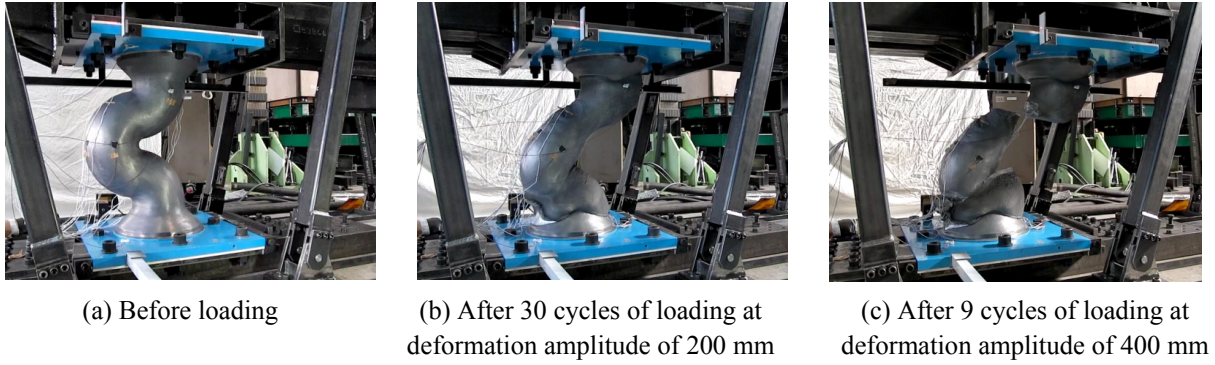
### 3.2. Results of the Lead Damper Tests

Photograph 3.1 shows changes in the shape of specimen 1 due to the cyclic shear loading. Specimen 1 was given 30 cycles of loading at shear deformation amplitudes of 100 mm and 200 mm and loading until breakage at a shear deformation amplitude of 400 mm. After 30 cycles of loading at deformation amplitude of 200 mm (Photograph 3.1 (b)), a crack appeared under the convex part of the lead damper. Breakage occurred at the ninth cycle of the loading at a shear deformation amplitude of 400 mm above the convex part of the lead damper (Photograph 3.1 (c)). Fig. 3.4 (a) shows shear force-deformation hysteresis loops obtained from the test for specimen 1. The lead damper exhibited degradation of the yield shear strength with the increase in the number of loading cycles. The loops at shear deformation amplitudes of 200 mm and 400 mm are not symmetric. These behaviours in the experimental hysteresis loops are due to changes in the shape of the lead damper. Fig. 3.4 (b) shows variations of the yield shear strength depending upon the accumulative shear deformation that the lead damper experienced. The yield shear strength,  $Q_y$ , is calculated from the following equation:

$$Q_y = \frac{W}{2(d_{\max} - d_{\min} - d_y)} \quad (3.1)$$

where  $W$  is absorbed energy per one cycle hysteresis loop,  $d_{\max}$  and  $d_{\min}$  are the peak displacement on one cycle hysteresis loop in plus and minus side, respectively and  $d_y$  is yield displacement. In Fig. 3.4 (b),  $Q_y$  is expressed in terms of its ratio to the third cycle loop.  $Q_y$  declined with the increase in accumulative deformation. However,  $Q_y$  showed a temporary rise when the deformation amplitude was changed. The yield shear strength at breakage was 45 % of that at the third cycle loop of the test.

Fig. 3.5 shows shear force-deformation hysteresis loops obtained from the cyclic loading tests in the direction of P for the first time, O and P for the second time for specimen 2. The hysteresis loops obtained from 30 cycles of loading in the direction of O (Fig. 3.5 (b)) is similar to that obtained from 30 cycles of loading in the direction of P for the first time (Fig. 3.5 (a)). On the other hand, the hysteresis loops obtained from cyclic loading in the direction of P for the second time (Fig. 3.5 (c)) show larger yield strength, about 350 kN, than that in the direction of P for the first time. It appears



**Photograph 3.1.** Variation in the appearance of specimen 1 due to cyclic shear loading

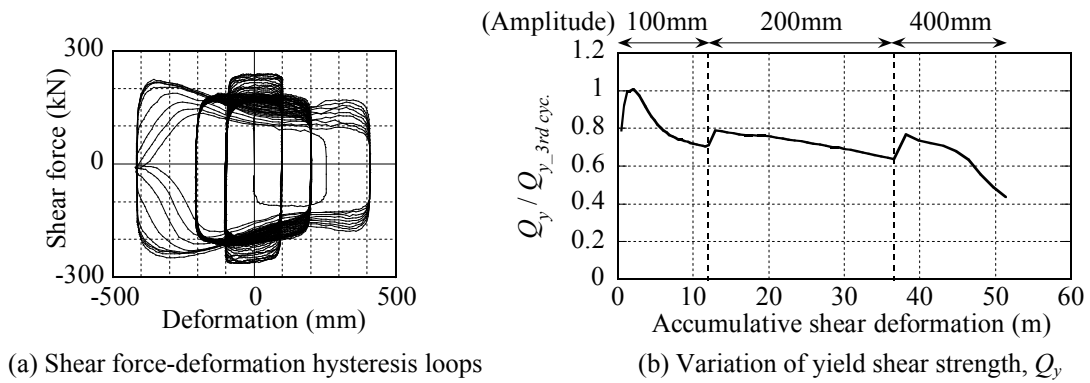


**Figure 3.4.** Experimental hysteresis loops and variation of yield shear strength of specimen 1

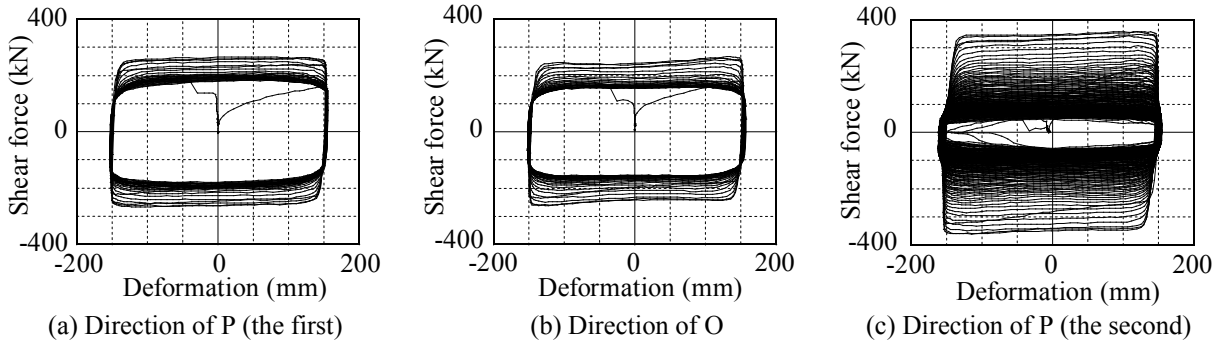


**Figure 3.5.** Shear force-deformation hysteresis loops of specimen 2

that the larger yield shear strength in the experimental hysteresis loops in the second direction of P is due to changes in the shape of the lead damper caused by cyclic loading in the direction of O.

Fig. 3.6 shows shear force-deformation hysteresis loops obtained from random loading tests using response displacement motions at the isolation layer. The yield shear strength in the experimental hysteresis loops after the fourth time loading (Fig. 3.6 (b)) in comparison with that from the first to third time (Fig. 3.6 (a)) is obviously small. Accumulative shear deformation, accumulative absorbed energy and variation in absorbed energy per one time loading are shown in Table 3.2. Accumulative shear deformation that specimen 3 experienced is above 160 m. Specimen 3 kept absorbing energy by the end of the loading and absorbed energy of a total of 17,755 kNm. However, the lead damper significantly deforms its shape at the twelfth time of loading as shown in Photograph 3.2. The absorbed energy at sixth time of loading was the least and about 44 % of that at the first time of loading.

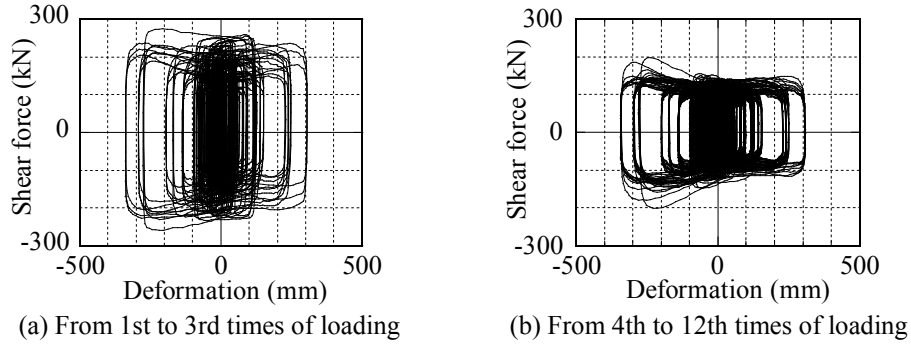


**Figure 3.6.** Shear force-deformation hysteresis loops of specimen 3

**Table 3.2.** Accumulative shear deformation and absorbed energy of specimen 3

Loading time	$\Sigma D$ (m)	$\Sigma W$ (kNm)	$W$ (kNm)	$W / W_{1st}$
1	13.1	2494	2494	1.000
2	26.3	4623	2129	0.853
3	39.8	6366	1743	0.699
4	53.4	7883	1517	0.608
5	67.0	9070	1187	0.476
6	80.7	10158	1088	0.436
7	94.4	11249	1091	0.437
8	108.2	12416	1167	0.468
9	121.9	13698	1281	0.514
10	135.6	15047	1349	0.541
11	149.2	16403	1357	0.544
12	162.9	17755	1352	0.542

$\Sigma D$ : Accumulative shear deformation,  $\Sigma W$ : Accumulative absorbed energy

$W$ : Absorbed energy per one time loading at response displacement

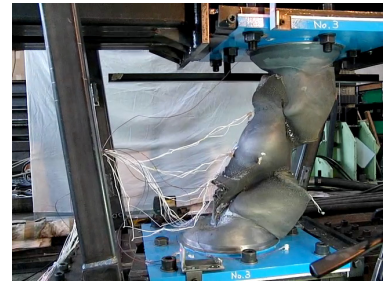
$W_{1st}$ : Absorbed energy of the first time loading at response displacement



(a) The first time



(b) The third time



(c) The twelfth time

**Photograph 3.2.** Variation in the appearance of specimen 3 at the peak displacement

### 3.3. Fatigue Characteristics of Lead Damper

In this section, the cumulative fatigue damage of the lead damper is evaluated. The number of cycles until breakage of the lead damper is calculated from the following equation:

$$N_f = 8.84 \times 10^5 \times \delta^{-1.74} \quad (3.2)$$

where  $N_f$  is number of cycles until breakage at a certain deformation amplitude and  $\delta$  is shear deformation amplitude. Eqn. 3.2 is an empirical formula derived from results of cyclic shear loading tests at constant shear deformation amplitudes of 20 mm to 800 mm. The number of cycles at random shear loading for specimen 3 is calculated using the rain flow method. Cumulative fatigue damage,  $D$ , is calculated from Eqn. 2.4. Fig. 3.7 shows cumulative fatigue damage,  $D$ , for specimens 1 and 3.

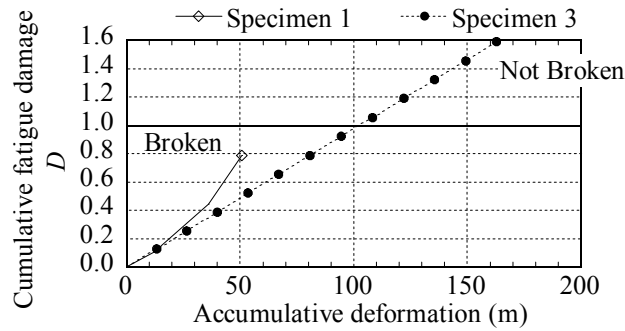


**Figure 3.7.** Cumulative fatigue damage,  $D$ , related to accumulative deformation

Although  $D=0.788$ , which is below 1.0, specimen 1 broke, whereas specimen 3 did not break at the time  $D$  was over 1.0. Because there was not a lot of cycle at peak deformation amplitude in random loading, continuous sinusoidal loading for specimen 1 was a more severe loading case than random loading for specimen 3.

#### 4. CONCLUSION

Multi-cyclic loading tests of full-scale steel dampers and lead dampers were conducted in order to investigate the performance of these dampers against long-period earthquake motions. The hysteretic behaviours of the steel dampers tested were stable until the damper rods achieved their fracture. The steel dampers exhibited a gradual decline in the yield shear strength with the increase in the number of loading cycles and the breakage of a damper rod caused a reduction in the absorbed energy. Comparing the test results and the existing expression for fatigue damage lead to the conclusion that the number of cycles until the damper rod was broken can be predicted by the existing expression for cumulative fatigue damage and Miner's rule. The lead dampers tested kept absorbing energy by the end of the loading. During loading, the lead dampers showed degradation of the yield shear strength and deformed its shape with the increase in accumulative shear deformations. The hysteretic behaviours of the lead dampers were influenced by shear deformation amplitude and changes in the shape caused by the cyclic loading. The lead damper given sinusoidal shear loading broke with less accumulative deformation than that the lead damper given random shear loading, which did not break, had experienced. The result indicates that the continuity of loading affects the fracture of the lead damper. In order to verify the safety of seismically isolated buildings against long-period earthquake motions, the feature mentioned above needs to be considered.

#### AKNOWLEDGEMENT

This paper describes a part of productions of the promotion project for building-standards maintenance "27-3 Examination about the safety verification method of the seismic isolated buildings against long-period ground motions" conducted by the Ministry of Land, Infrastructure, Transport and Tourism in the Heisei 22 fiscal year. Gratitude is respectfully expressed to the main committee (chairperson: Professor Haruyuki Kitamura of Tokyo University of Science), WG for testing of devices (chief examiner: Professor Mineo Takayama of Fukuoka University), WG for evaluation of response of buildings (chief examiner: Professor Takeshi Furuhashi of Nihon University) and all the persons concerned.

#### REFERENCES

- [1] S.S.Manson. (1966). Thermal stress and low-cycle fatigue, McGraw-Hill, New York, U.S.
- [2] M.A.Minor. (1945). Cumulative Damage in Fatigue. *Journal of Applied Mech.* **Vol.2**, A159-A164.